

## PREDICTION OF BOUNDARY LAYER THICKNESS AND FRICTION VELOCITY BY SYMMETRY ARGUMENTS

Chenning Tong

Department of Mechanical Engineering  
Clemson University  
Clemson, South Carolina 29631  
ctong@clemson.edu

### ABSTRACT

We derive analytically for the first time the downstream evolution of the boundary layer thickness and the friction velocity of the zero-pressure-gradient turbulent boundary layer (ZPGTBL). Lie groups were used to derive the downstream evolution and to obtain the full set of the similarity variables and the leading-order similarity equations. An approximate leading-order solution was obtained using matched asymptotic expansions. The similarities and differences between ZPGTBL and turbulent channel flows in terms of the similarity equations are discussed to support the notion of leading-order universality of the near-wall layer.

### INTRODUCTION

The zero-pressure-gradient turbulent boundary layer (ZPGTBL) is one of the most important flows to understand the fundamental physics of turbulence, and has been studied extensively (e.g., Prandtl (1925); von Kármán (1930); Klebanoff (1954); Schlichting (1956); Clauser (1956); Monin & Yaglom (1971); Sreenivasan (1989); Pope (2000); McKeon & Sreenivasan (2007); Nagib *et al.* (2007); Marusic *et al.* (2010); Smits *et al.* (2011)). Essential to the understanding of a boundary layer is its similarity solution. The zero-pressure-gradient laminar boundary layer (the Blasius boundary layer, Blasius (1908)) has the well-known similarity solution, a key part of which is the downstream evolution of the boundary layer thickness and the surface stress.

Over the past decades there have been many efforts devoted to finding a similarity solution of ZPGTBL. Tennekes & Lumley (1972) obtained a leading-order mean momentum similarity equation. Mellor (1972) obtained the log law. However, prediction of the boundary layer thickness and the wall shear stress has proven to be much more challenging and has not been made successfully. Tennekes & Lumley (1972) used the boundary layer thickness  $\Delta$  defined by Clauser (1956) using an integral quantity, not derived from the boundary layer parameters, in contrast to that of the Blasius boundary layer. Its downstream evolution and the friction velocity were not predicted, preventing a proper definition of the similarity variables. A Lie group analysis was performed in Oberlack & Khujadze (2006) to find a linear growth of the boundary layer thickness, which is inconsistent with experimental evidence (e.g., Marusic *et al.* (2015)). The same definition of  $\Delta$  as Tennekes & Lumley (1972) was used in Monkewitz *et al.* (2007), but did not provide an expression for it. The analysis in George & Castillo (1997) attempted to obtain a similarity solution us-

ing the Reynolds-averaged boundary layer equations without the viscous terms. However, as we show in this work, their velocity scale for the outer layer is incorrect. Without a prediction of the boundary layer thickness (and the friction velocity), the similarity variables cannot be properly defined. The existence of a similarity solution and boundary layer similarity also cannot be shown.

In this work we perform a symmetry analysis of the Reynolds-averaged boundary layer equations to derive analytically for the first time the evolution of the boundary layer thickness,  $\delta$ , whose definition is not predetermined and will come from the analysis, the evolution of the friction velocity, the full set of similarity variables, and the (ordinary differential) similarity equations. We then employ the method of matched asymptotic expansions to obtain an approximate solution.

Parallel to the research on ZPGTBL, there also have been much effort to investigate turbulent channel and pipe flows, which are amenable to more rigorous asymptotic analysis (e.g., Millikan (1938); Afzal (1976)). The near-wall (or inner) layers of these flows are widely believed to have much in common, i.e., the near-wall layers are universal. There is also evidence against universality (e.g., McKeon & Morrison (2007); Nagib *et al.* (2007); Marusic *et al.* (2015)). However, there have been essentially no theoretical analyses on the similarities and differences between these flows. The present work will also help shed some light on the important issue of the universality of the near-wall layers.

### SYMMETRIES

Symmetries of differential equations refer to form invariance of the equations under group transformations, and can be exploited to help obtain solutions of the equations. One of the symmetries of the Navier-Stokes equations is invariance under a one-parameter Lie dilation group (e.g., Bluman & Kumei (1989); Cantwell (2002)). A key requirement for this invariance is a fixed Reynolds number. However, it has long been recognized that statistics of the energy-containing eddies in turbulent flows at high Reynolds numbers are approximately Reynolds number invariant. This approximate invariance is associated with spontaneous breaking of the symmetries of the Navier-Stokes equations from laminar to turbulent flows. Therefore, while the symmetries of laminar flows are exact, the symmetries of turbulent flows are only approximate. The concept of spontaneous symmetry breaking and approximate symmetry first emerged in condensed matter physics and later

were key to predicting certain non-zero mass particles in Yang-Mills gauge fields (Higgs (1964, 2014); Castellani (2003)). In the present work, we seek the leading-order symmetries and similarity properties of ZPGTBL. Therefore, Reynolds number invariance of energy-containing statistics is invoked as the (only) physical assumption.

We use Lie dilation groups to analyze the leading-order symmetries (group transformation properties) of the ZPGTBL equations: the mean momentum equation, the Reynolds stress budget, and the mean continuity equation. The groups will be used to derive the evolution of the boundary layer thickness and the Reynolds shear stress and to obtain the similarity variables.

To obtain the leading-order symmetries, we recognize that the outer layer is approximately Reynolds number independent and whereas the inner layer depends on the viscosity. Therefore, we need to derive the leading-order equations for the two layers and analyze their symmetries separately.

### OUTER-LAYER SYMMETRY

For the outer layer, the leading-order symmetries (or the symmetries of the leading-order equations) can be obtained by dropping the Reynolds-number-dependent terms. These symmetries are similar in nature to the approximate symmetries previously investigated (e.g., Grebenev & Oberlack (2007)). It is easily shown that by dropping the viscous term in the mean momentum equation, as done by George & Castillo (1997), the group leads to a boundary layer thickness  $\delta \propto x$  and  $\overline{w} = const.$ , inconsistent with the behaviors of ZPGTBL. The reason is that there are other higher-order terms in the equations that do not contain the viscosity, but are implicitly Reynolds-number dependent. They also need to be identified and dropped.

To identify the higher-order terms, we perform an order of magnitude analysis of the boundary layer equations. The mean momentum equation is

$$U \partial_x U + V \partial_y U = -\partial_y \overline{w} - \partial_x (\overline{u^2} - \overline{v^2}) + \nu \partial_y^2 U, \quad (1)$$

where  $U$ ,  $V$ ,  $\overline{w}$ ,  $\overline{u^2}$ ,  $\overline{v^2}$ ,  $\nu$ , and  $y$  are the streamwise and normal mean velocity components, the Reynolds shear stress, the Reynolds normal stress components, the kinematic viscosity, and the wall-normal coordinate, respectively ( $x$  and  $z$  are the streamwise and spanwise coordinates respectively and  $u$ ,  $v$  and  $w$  are the corresponding velocity fluctuations respectively hereafter). The Reynolds shear stress budget is

$$U \partial_x \overline{w} + V \partial_y \overline{w} = -\overline{u \partial_y p} - \overline{v \partial_x p} - \overline{v^2} \partial_y U - \partial_y \overline{uv^2} + \nu \partial_y^2 \overline{w} - \varepsilon_{uv}, \quad (2)$$

where  $\varepsilon_{uv}$  is the dissipation rate, which is generally negligible. The TKE budget is

$$U \partial_x k + V \partial_y k = -\overline{w} \partial_y U - \partial_y \overline{p} - \partial_y (\overline{u^2} + \overline{v^2} + \overline{w^2}) \nu / 2 + \nu \partial_y^2 k - \varepsilon, \quad (3)$$

where  $\varepsilon$  is the TKE dissipation rate. We first consider the scaling of the velocity defect  $U - U_e \sim U_e$  proposed in George & Castillo (1997), where  $U$  and  $U_e$  are the mean streamwise velocity and the free-stream velocity respectively. With this scaling, the Reynolds shear stress and the shear production of the turbulent kinetic energy (TKE) would scale as  $-\overline{w} \sim U_e^2 \delta / L$  and  $-\overline{w} \partial_y U \sim U_e^3 / L$  respectively, where  $L \sim x$  is the streamwise length scale. Since shear production is the only pro-

duction mechanism, the TKE would scale as  $k \sim U_e^2$ . According to Taylor's scaling (Taylor 1935), which follows from the Reynolds-number invariance assumption, the dissipation would scale as  $k^{3/2} / \delta \sim U_e^3 / \delta$ , asymptotically larger than the production, indicating that the scaling  $U - U_e \sim U_e$  is inconsistent with the scaling of the dissipation, unless  $\delta / L = const.$  However, a linear growth of  $\delta$  is inconsistent with experimental evidence. Here we will also show that  $\delta / L \neq const.$  We consider the mean momentum integral

$$-u_*^2 = \frac{d}{dx} \int_0^\infty U(U - U_e) dy. \quad (4)$$

As both  $U$  and  $U - U_e$  scale with  $U_e$ , the momentum integral results  $u_*^2 \sim U_e^2 \delta / L \sim \overline{w}$ . With  $U_e$  and  $u_*$  as the outer and inner velocity scales respectively, asymptotic matching of the outer and inner expansions of the mean velocity profile (assuming existence of a similarity solution) gives

$$y^+ \frac{dU^+}{dy^+} = \frac{U_e}{u_*} y_o \frac{dU_o}{dy_o} \sim \left(\frac{L}{\delta}\right)^{1/2} y_o \frac{dU_o}{dy_o}, \quad (5)$$

where  $y^+ = u_* y / \nu$ ,  $U^+ = U / u_*$ ,  $y_o = y / \delta$ , and  $U_o = (U - U_e) / U_e$ . Therefore,

$$(y^+)^{\alpha} = \left(\frac{L}{\delta}\right)^{1/2} y_o^{\alpha} = \left(\frac{L}{\delta}\right)^{1/2} (Re_*^{-1} y^+)^{\alpha}. \quad (6)$$

Reynolds number invariance requires

$$\left(\frac{\delta}{L}\right)^{1/2} Re_*^{\alpha} = const. \quad (7)$$

As the outer and inner velocity scales are different, the velocity profile in the matching layer cannot be logarithmic, resulting in  $\alpha \neq 0$  and  $Re_*^{\alpha} = (u_* \delta / \nu)^{\alpha} \neq const.$ . Therefore  $\delta / L \neq const.$ , indicating that the scaling choice  $U - U_e \sim U_e$  is inconsistent with the scaling of the dissipation rate. Furthermore, it can be shown using the mean momentum integral that  $U - U_e \sim u_*$  and  $\partial U / \partial y \sim u_* / \delta$ .

With  $U - U_e \sim u_*$ , we perform an order of magnitude analysis to identify the leading-order terms in the equations, which are Reynolds number invariant. The resulting leading-order mean momentum equation is

$$U_e \partial_x U = -\partial_y \overline{w}. \quad (8)$$

Similarly we obtain the leading-order shear stress budget and TKE budget,

$$U_e \partial_x \overline{w} = -(\overline{u \partial_y p} + \overline{v \partial_x p}) - \overline{v^2} \partial_y U. \quad (9)$$

$$U_e \partial_x k = -\overline{w} \partial_y U - \partial_y \overline{p} - \partial_y (\overline{u^2} + \overline{v^2} + \overline{w^2}) \nu / 2 - \varepsilon. \quad (10)$$

The velocity-pressure gradient term in the shear stress budget scales the same as production. The pressure transport and turbulent transport terms in the TKE budget scale the same as

production. Therefore, they should dilate in the same way as the production terms. The finite form of the dilation group is

$$\begin{aligned}\tilde{x} &= e^a x, \quad \tilde{y} = e^b y, \quad \tilde{U} = U, \quad \tilde{U} - U_e = e^g (U - U_e), \\ \partial \tilde{U} &= e^g \partial U, \quad \tilde{V} = e^c V, \quad \tilde{\overline{uv}} = e^{d_2} \overline{uv}, \quad \tilde{\overline{u^2}} = e^{d_1} \overline{u^2}, \quad \tilde{\overline{v^2}} = e^{d_1} \overline{v^2}.\end{aligned}\quad (11)$$

where  $a, b$  etc., are the group parameters. For the equations to be invariant the exponents must satisfy  $g - a = d_2 - b$ ,  $d_2 - a = d_1 + g - b$ , and  $d_1 - a = d_2 + g - b = 3d_1/2 - b$ , respectively, leading to  $d_2 = d_1 = 2b - 2a$  and  $g = b - a$ , and hence a two-parameter dilation group.

To obtain a one-parameter group an additional relationship is needed. Since the outer and inner layers are linked, this relationship must come from asymptotically matching the outer layer with the inner layer. However, at this point we do not have similarity equations, and cannot yet perform matching. Nevertheless, assuming that a similarity solution exists, matching the two layers with identical velocity scales ( $u_*$ ) would result in a logarithmic velocity profile and a logarithmic friction law. Therefore, we use the logarithmic friction law as an ansatz to provide this relation. We will show later that the group and the subsequent analysis indeed lead to the logarithmic friction law and that the similarity solution in the matching layer satisfies the mean momentum equation. This essentially amounts to guessing the solution of an equation and verifies it later using the equation. The friction law dilates as

$$\frac{U_e}{u_* e^g} = \frac{1}{\kappa} \ln \frac{u_* \delta e^{g+b}}{v} + D = \frac{1}{\kappa} \left( \ln \frac{u_* \delta}{v} + g + b \right) + D. \quad (12)$$

Note that  $\delta$  as a function of  $x$  is not yet known, and therefore is not fully defined. Since (12) is invariant under the dilation group, we have

$$\frac{U_e}{u_*} = e^g \left\{ \frac{1}{\kappa} \left( \ln \frac{u_* \delta}{v} + g + b \right) + D \right\} = \frac{1}{\kappa} \ln \frac{u_* \delta}{v} + D. \quad (13)$$

Therefore

$$(e^g - 1) \left\{ \frac{1}{\kappa} \ln \frac{u_* \delta}{v} + D \right\} = (e^g - 1) \frac{U_e}{u_*} = -\frac{g+b}{\kappa} e^g. \quad (14)$$

This equation provides an implicit relationship between  $g$  and  $b$ . Rather than directly solving (14) we examine infinitesimal form of the group with exponents  $dg, da$ , and  $db$  etc. Taylor expanding the second and third terms in (14) and keeping the leading-order terms we have

$$dg \frac{U_e}{u_*} = -\frac{dg+db}{\kappa} \quad \text{or} \quad dg = \frac{-db}{\kappa \frac{U_e}{u_*} + 1} = \frac{-da}{\kappa \frac{U_e}{u_*} + 2}. \quad (15)$$

From the continuity equation, we have  $dg - da = dc - db$ ,  $dc = 2dg$ . We obtain a one-parameter group

$$\begin{aligned}\tilde{x} &= e^{da} x, \quad \tilde{y} = e^{db} y, \quad \tilde{U} - U_e = e^{dg} (U - U_e), \quad \tilde{V} = e^{2dg} V, \\ \tilde{\overline{uv}} &= e^{2dg} \overline{uv}, \quad \tilde{\overline{u^2}} = e^{2dg} \overline{u^2}, \quad \tilde{\overline{v^2}} = e^{2dg} \overline{v^2}, \quad \tilde{u}_* = e^{dg} u_*.\end{aligned}\quad (16)$$

Note that  $\delta$  dilates in the same way as  $y$ . From (16) we obtain the characteristic equations of the group

$$\begin{aligned}\frac{du_*}{u_*} &= -\frac{dy}{y(\kappa \frac{U_e}{u_*} + 1)} = -\frac{d\delta}{\delta(\kappa \frac{U_e}{u_*} + 1)} = -\frac{dx}{x(\kappa \frac{U_e}{u_*} + 2)} \\ &= \frac{d(U - U_e)}{U - U_e} = \frac{dV}{2V}.\end{aligned}\quad (17)$$

From the first and fourth terms we obtain (without the dimensional integration constant)  $x \sim u_*^{-2} e^{\kappa U_e/u_*}$ . Its non-dimensional form is

$$U_e x/v = Re_x \sim (U_e^2/u_*^2) e^{\kappa U_e/u_*}. \quad (18)$$

Similarly we obtain  $\delta \sim u_*^{-1} e^{\kappa U_e/u_*}$ ,  $V \sim u_*^2$ . The non-dimensional form of  $\delta$  is

$$U_e \delta/v = Re_\delta \sim (U_e/u_*) e^{\kappa U_e/u_*}. \quad (19)$$

Equations (18) and (19) are functions of  $U_e/u_*$  which can be used as a parameter to obtain the dependence of  $\delta$  on  $x$ . These are the central results of the present work and to our best knowledge, are the first analytic derivation of the downstream evolution of the friction velocity and the boundary layer thickness.

The first and last two terms in (17) result in  $U - U_e \sim u_*$  and  $V \sim u_*^2$ . Non-dimensionalizing the variables using  $x, u_*$  and  $U_e$ , we obtain for the first time the full set of the similarity variables for the outer layer  $U_o = (U - U_e)/u_*$ ,  $V_o = V U_e/u_*^2$ ,  $y_o = y U_e/(x u_*)$ ,  $\overline{uv}_o = \overline{uv}/u_*^2$ ,  $\overline{u^2}_o = \overline{u^2}/u_*^2$ ,  $\overline{v^2}_o = \overline{v^2}/u_*^2$ . Here  $y_o$  is defined using the boundary layer parameters ( $x, U_e$ , and  $u_*$ ), in a similar way to the Blasius boundary layer.

## INNER-LAYER SYMMETRY

We now perform a Lie group analysis of the leading-order inner equations. The leading-order mean momentum equation is Tennekes & Lumley (1972)

$$0 = -\partial_y \overline{uv} + \nu \partial_y^2 U. \quad (20)$$

The dilation group is  $\tilde{y} = e^b y$ ,  $\tilde{U} = e^g U$ ,  $\tilde{\overline{uv}} = e^{2g} \overline{uv}$ . The transformation for  $\overline{uv}$  is identical to the outer layer because it scales with  $u_*^2$  in both layers. For (20) to be invariant, the exponents must satisfy  $2g - b = g - 2b$ ,  $b = -g$ . From the continuity equation, we have  $g - a = c - b$ ,  $c = -a$ . These group parameters are also consistent with the dilation properties of the Reynolds shear stress and TKE budgets. The group now is

$$\tilde{x} = e^a x, \quad \tilde{y} = e^{-g} y, \quad \tilde{U} = e^g U, \quad \tilde{V} = e^{-a} V, \quad \tilde{\overline{uv}} = e^{2g} \overline{uv}, \quad (21)$$

where  $a$  and  $g$  are related by (14). The characteristic equations for the group are

$$\frac{du_*}{u_*} = -\frac{dy}{y} = -\frac{dx}{x(\kappa \frac{U_e}{u_*} + 2)} = \frac{dV}{V(\kappa \frac{U_e}{u_*} + 2)}. \quad (22)$$

The first two terms result in  $u_* \sim y^{-1}$ . The last two terms lead to  $V \sim x^{-1}$ . We obtain the similarity variables for the inner layer  $U_i = U/u_*$ ,  $V_i = Vx/v$ ,  $y_i = yu_*/v = y^+$ ,  $\overline{uv}_i = \overline{uv}/u_*^2$ ,  $\overline{u_i^2} = \overline{u^2}/u_*^2$ ,  $\overline{v_i^2} = \overline{v^2}/u_*^2$ , where  $V_i$  has not been properly defined previously in the literature.

## APPROXIMATE SOLUTION USING MATCHED ASYMPTOTIC EXPANSIONS

In a typical Lie group analysis, after the symmetries are identified and the similarity variables are obtained, the similarity equations are derived and their solution is sought. In the case of turbulent flows, the similarity equations are unclosed and generally cannot be solved without a turbulence model. However, matching the outer and inner asymptotic expansions provides additional relations, allowing us to obtain an approximate solution without a turbulence model.

We write the outer layer similarity variables as asymptotic expansions

$$\begin{aligned} U_o(y_o, Re_*) &= U_{o1}(y_o) + \text{higher-order terms}, \\ \overline{uv}_o(y_o, Re_*) &= \overline{uv}_{o1}(y_o) + \text{higher-order terms}, \end{aligned} \quad (23)$$

where the similarity variables  $U_{o1}$  etc. are of order one. Substituting (23) into the mean momentum equation, we obtain the leading-order similarity equation for  $U_o$

$$-y_o d_{y_o} U_{o1} = -d_{y_o} \overline{uv}_{o1}, \quad (24)$$

which is identical to that obtained by Tennekes & Lumley (1972). However, their definition of  $y_o$  is different. Similarly, the leading-order shear-stress budget is

$$-y_o d_{y_o} \overline{uv}_{o1} = -\overline{(u\partial_y p + v\partial_x p)}_o - \overline{v_o^2} d_{y_o} U_{o1}. \quad (25)$$

Since the outer expansions are not valid in the viscous region (the inner layer), inner expansions are also needed.

The inner similarity variables depend on  $y^+$  and  $Re_*$ . We write them as asymptotic expansions,

$$\begin{aligned} U_i(y^+, Re_*) &= U_{i1}(y^+) + \text{higher-order terms}, \\ \overline{uv}_i(y^+, Re_*) &= \overline{uv}_{i1}(y^+) + \text{higher-order terms}. \end{aligned} \quad (26)$$

We obtain the leading-order inner similarity equations

$$\begin{aligned} 0 &= -d_{y^+} \overline{uv}_i + d_{y^+}^2 U_i \\ 0 &= -\overline{(u\partial_y p + v\partial_x p)}_i - \overline{v_i^2} d_{y^+} U_{i1} + d_{y^+}^2 \overline{uv}_{i1} \end{aligned} \quad (27)$$

We now asymptotically match the outer and inner expansions

$$\begin{aligned} U &= U_e + u_* U_o = U_e + u_* U_{o1}(y_o) + \dots, \\ U &= u_* U_i = u_* U_{i1}(y^+) + \dots, \end{aligned} \quad (28)$$

for  $y_o \ll 1$  and  $y^+ \gg 1$ , resulting the log law (see e.g., Tong & Ding (2020) for details)

$$U_{o11} = \frac{1}{\kappa} \ln y_o + C, \quad U_{i11} = \frac{1}{\kappa} \ln y^+ + B, \quad (29)$$

where  $U_{o11}$  and  $U_{i11}$  are the leading-order expansions of  $U_{o1}$  and  $U_{i1}$ , respectively. Inserting (29) into (28) we obtain the dimensional outer and inner expansion as

$$U = U_e + u_* \left\{ \frac{1}{\kappa} \ln y_o + C + \dots \right\}, \quad U = u_* \left\{ \frac{1}{\kappa} \ln y^+ + B + \dots \right\}. \quad (30)$$

From (30) we obtain the logarithmic friction law

$$\frac{U_e}{u_*} = \frac{1}{\kappa} \ln \frac{y^+}{y_o} + B - C = \frac{1}{\kappa} \ln \frac{u_*^2 x}{U_e v} + B - C. \quad (31)$$

Using (18) and (19) we have  $\delta \sim xu_*/U_e$ . The friction law can then be written as (5), confirming the ansatz. Similarly we obtain the matching results for the leading-order Reynolds shear stress as  $\overline{uv} = u_*^2(-1 + y_o/\kappa)$ . One can also write down the expansions for the velocity-pressure-gradient terms and obtain matching results (not done here). With (18) and (19) and the fully defined similarity variables, (30) and  $\overline{uv} = u_*^2(-1 + y_o/\kappa)$  satisfy (1) to the leading order, verifying them (and 12) as part of a similarity solution of the ZPGTBL equations. Furthermore, from a mathematical point of view, the boundary layer equations and their boundary conditions are a well-posed problem, therefore have a unique solution. Physically, the evolution of ZPGTBL is also unique. Hence the ansatz has led to the unique similarity solution, fully justifying its use. The solution also provide the downstream variations of the mean velocity and shear stress profiles, which previously were not available.

We now make preliminary comparisons of the theoretical prediction (18) and (19) of the non-dimensional velocity  $U_e/u_*$  (equivalent to the surface shear stress) and the non-dimensional outer layer thickness  $Re_\delta = U_e \delta_{99}/v$  (both as functions of the non-dimensional downstream distance  $Re_x = U_e x/v$ ) with the experimental data of Marusic *et al.* (2015) (the SP40 configuration). The measured values of  $U_e/u_*$  are used as the parameter to obtain the theoretical values of  $Re_x$  and  $Re_\delta$ . The theoretical prediction contains several non-dimensional coefficients that need to be obtained using experimental data: The von Kármán constant  $\kappa = 0.420$  and the non-dimensional coefficient for  $\delta_{99}$  are obtained by fitting (19) to the experimental data; The virtual origin of  $x = -1.744$  m and the non-dimensional coefficient for  $Re_x$  are then obtained by fitting (18) to the data. In particular, the values of  $U_e/u_*$  and  $\delta_{99}$  at  $x = 1.6$  m are used to determine the non-dimensional coefficients. The kinematic viscosity is taken as the value in Marusic *et al.* (2015),  $\nu = 15.1 \times 10^{-6}$  m<sup>2</sup>/s. The results are

$$Re_x = 0.06024 \frac{U_e^2}{u_*^2} e^{\kappa U_e/u_*}, \quad Re_\delta = 0.02204 \frac{U_e}{u_*} e^{\kappa U_e/u_*}. \quad (32)$$

We then have  $\delta_{99} = 0.3659xu_*/U_e$ ,  $y_o = 0.3659y/\delta_{99}$ .

Figures 1 and 2 show that with these coefficients, the analytic prediction, especially the functional form, has an excellent agreement with the experiments. However,  $\kappa = 0.420$  obtained here based on the boundary layer thickness and the friction velocity, which are global behaviors, is quite different from 0.384 obtained in the same experiment and by Nagib *et al.* (2007) using the mean velocity profile, a local behavior, but is much closer to that of Vallikivi *et al.* (2015) (0.40) and the typical value of 0.421 in pipe flows (McKeon *et al.* (2004); McKeon & Morrison (2007)). We emphasize that these are preliminary comparisons with a single experiment. It is therefore unclear whether the different values are a coincidence or

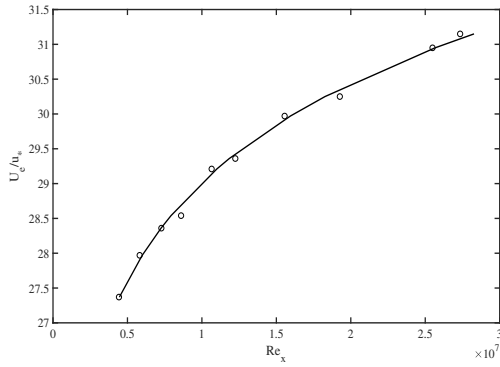


Figure 1.  $U_e/u_*$  vs. the non-dimensional downstream distance  $Re_x = U_e x/\nu$ . Circles: experimental data from Marusic (2015) (the SP40 configuration); Solid line: Theoretical prediction given by equation (32).

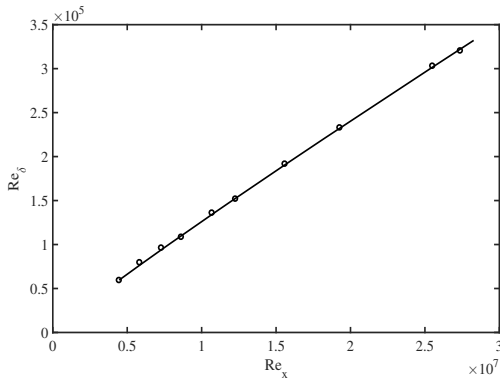


Figure 2. Non-dimensional boundary layer thickness  $Re_\delta = U_e \delta/\nu$  vs.  $Re_x$ . Legend same as in figure 1.

an indication of the differences in the two ways of estimating the von Kármán. This issue requires further attention in future studies.

### UNIVERSALITY OF NEAR-WALL LAYER

The leading-order equations allow us to compare ZPGTBL with channel flows to examine the key question of near-wall universality. In the inner layer the mean momentum equation is dominated by the Reynolds stress and viscous stress terms (Afzal (1976) and equation 27) in both flows. The Reynolds shear stress budgets also have similar properties in both flows, being dominated by the production, pressure, and viscous terms (Hoyas & Jimenes (2008) and equation 27). The similarity variables are also defined in the same way, indicating that the two flows have the same leading-order structure.

This issue can be further examined using the outer equations. In channel flows, the Reynolds shear stress budget is a balance between shear production and velocity-gradient–pressure interaction (Hoyas & Jimenes (2008)). The mean velocity gradient is “adjusted” to balance the Reynolds stress budget. The leading-order mean momentum equation is a balance between the shear stress derivative and the mean pressure gradient (Afzal (1976)), with the latter imposing the linear variation of the leading-order (linear) variation of the Reynolds shear stress.

In ZPGTBL the Reynolds shear stress balance (equa-

tion 25) is among the mean advection, production and velocity gradient–pressure interaction. However, in the log layer ( $y_o \ll 1$ ), the advection term is of higher-order. Therefore the balance in the log layer is asymptotically identical to that in channel flows. While the mean momentum balance (24) is between the mean advection and the shear stress derivative, the log law ensures the leading-order (linear) variation of the Reynolds shear stress. Therefore, from the perspective of both the inner and outer equations, the leading-order near-wall structure of channel flows and ZPGTBL are the same, supporting the notion of universality of the leading-order near-wall turbulence. The differences observed in experiments are potentially due to higher-order effects, which deserve further attention.

### CONCLUSIONS

We performed a symmetry analysis of the equations for ZPGTBL using Lie dilation groups, and obtained local, leading-order symmetries of the equations. We derived for the first time the evolution of the boundary layer thickness and the shear stress, and the full set of similarity variables. Using the asymptotic expansions the leading-order similarity equations for the outer and inner layers were obtained. Matching the expansions resulted in an approximate similarity solution in the overlapping layer, the log law. The leading-order equations for both the channel flows and ZPGTBL show similar properties in the near wall layer, supporting the notion of its universality.

### ACKNOWLEDGMENTS

The author thanks Professors Katepalli Sreenivasan for encouraging him to look into issues in classical engineering turbulent boundary layers and for providing valuable comments on the manuscript. This work was supported by the National Science Foundation under grant AGS-2054983.

### REFERENCES

- Afzal, N. 1976 Millikan’s argument at moderately large reynolds number. *Phys. Fluids* **19**, 600–602.
- Blasius, H. 1908 Grenschichten in flussigkeiten mit kleiner reibung. *Z. Math. Phys.* **56**, 1–37.
- Bluman, G. W. & Kumei, S. 1989 *Symmetry and differential equations*. New York, USA: Springer.
- Cantwell, B. J. 2002 *Introduction to symmetry analysis*. Cambridge, UK: Cambridge University Press.
- Castellani, E. 2003 On the meaning of symmetry breaking. In *Symmetries in physics: philosophical reflections*, pp. 1–17. Cambridge University Press.
- Clauser, F. H. 1956 The turbulent boundary layer. *Adv. Appl. Mech.* **56**, 1–51.
- George, W. K. & Castillo, L. 1997 Zero pressure gradient turbulent boundary layer. *Appl. Mech. Rev.* **50**, 689–729.
- Grebenev, V. N. & Oberlack, M. 2007 Approximate symmetries of the navier-stokes equations. *J. Nonlinear Math. Phys.* **14**, 157–163.
- Higgs, P. W. 1964 Broaken symmetries and the masses of gauge bosons. *Phys. Rev. Let.* **13**, 508–509.
- Higgs, P. W. 2014 Nobel lecture: Evading the goldstone theorem. *Rev. Modern Phys.* **86**, 851–853.
- Hoyas, S. & Jimenes, J. 2008 Reynolds number effects on the reynolds- stress budgets in turbulent channels. *Phys. Fluids* **20**, 101511.

- von Kármán, Theodore 1930 Mechanische Ähnlichkeit und Turbulenz. In *Proc. Third Int. Congr. Applied Mechanics*, pp. 85–105. Stockholm.
- Klebanoff, P. S. 1954 Characteristics of turbulence in a turbulent boundary layer with zero pressure gradient. *TN3178 NACA*.
- Marusic, I., Chauhan, K. A., Kulandaivelu, V. & Hutchins, N. 2015 Evolution of zero-pressure-gradient boundary layers from different tripping conditions. *Fluid Mech.* **783**, 379–411.
- Marusic, I., McKeon, B. J., Monkewitz, P. A., Nagib, H. M. & Smits, A. J. 2010 Wall-bounded turbulent flows at high reynolds numbers: Recent advances and key issues. *Phys. Fluids* **22**, 065103.
- McKeon, B. J., Li, J., Jiang, W., Morrison, J. F. & Smits, A. J. 2004 Further observations on the mean velocity distribution in fully developed pipe flow. *Fluid Mech.* **501**, 135–147.
- McKeon, B. J. & Morrison, J. F. 2007 Asymptotic scaling in turbulent pipe flow. *Philos. Trans. R. Soc. Lond. A* **365**, 771–787.
- McKeon, B. J. & Sreenivasan 2007 Introduction: scaling and structure in high reynolds number wall-bounded flows. *Philos. Trans. R. Soc. Lond. A* **365**, 635–646.
- Mellor, G. 1972 The large reynolds number, asymptotic theory of turbulent boundary layers. *Int. J. Eng. Sci.* **10**, 851–873.
- Millikan, Clark B. 1938 A critical discussion of turbulent flows in channels and circular tubes. *Proc. Fifth Int. Conference Appl. Mech.*
- Monin, A. S. & Yaglom, A. M. 1971 *Statistical Fluid Mechanics*. Cambridge, MA: MIT press.
- Monkewitz, P. A., Chauhan, K. A. & Nagib, H. M. 2007 Self-contained high reynolds-number asymptotics for zero-pressure-gradient turbulent boundary layers. *Phys. Fluids* **19**, 115101.
- Nagib, H. M., Chauhan, K. A. & Monkewitz, P. A. 2007 Approach to an asymptotic state for zero pressure gradient turbulent boundary layers. *Phil. Trans. R. Soc. Lond. A* **365**, 755–770.
- Oberlack, M. & Khujadze, G. 2006 Symmetry methods in turbulent boundary layer theory: New wake region scaling laws and boundary layer growth. In *IUTAM Symposium on One Hundred Years of Boundary Layer Research* (ed. G.E.A. Meier, K.R. Sreenivasan & Hans-Joachim. Heinemann), pp. 39–48. Springer.
- Pope, S. B. 2000 *Turbulent Flows*. Cambridge, UK: Cambridge University Press.
- Prandtl, Ludwig 1925 Bericht über die Entstehung der Turbulenz. *Z. Angew. Math. Mech* **5**, 136–139.
- Schlichting, H. 1956 *Boundary layer theory*. New York, New York: McGraw Hill book company.
- Smits, A. J., McKeon, B. J. & Marusic, I. 2011 High-reynolds number wall turbulence. *Annu. Rev. Fluid Mech.* **43**, 353–375.
- Sreenivasan, K. R. 1989 The turbulent boundary layer. In *Lecture Notes in Physics*, pp. 159–209. Springer.
- Taylor, G. I. 1935 Statistical theory of turbulence. i-iv. *Philos. Trans. R. Soc. Lond. A* **151**, 421–478.
- Tennekes, H. & Lumley, J. L. 1972 *A First Course in Turbulence*. Cambridge, MA: MIT press.
- Tong, C. & Ding, M. 2020 Velocity-defect laws, log law and logarithmic friction law in the convective atmospheric boundary layer. *J. Fluid Mech.* **883**, A36.
- Vallikivi, M., M., Hultmark & Smits, A. J. 2015 Turbulent boundary layers statistics at very high reynolds number. *J. Fluid Mech.* **779**, 371–389.